

# Following the flux of long-chain bases through the sphingolipid pathway in vivo using mass spectrometry<sup>S</sup>

Fernando Martínez-Montañés and Roger Schneider<sup>1</sup>

Department of Biology, University of Fribourg, 1700 Fribourg, Switzerland

**Abstract** Sphingolipids are essential components of the plasma membrane. Their synthesis is tightly controlled by regulatory proteins, which impinge on the rate-limiting step of the pathway, the condensation of serine and palmitoyl-CoA to long-chain base (LCB). The subsequent conversion of LCB to ceramide by ceramide synthase (CerS) is also tightly regulated, because both the accumulation of LCB as well as an excess of ceramide is toxic. Here we describe an in vivo assay to monitor the flux of LCB through the sphingolipid pathway in yeast. Cells are provided with nonnatural odd-chain sphingosine analogs, C17-dihydrosphingosine or C17-phytosphingosine (PHS), and their incorporation into ceramide and more complex sphingolipids is monitored by mass spectrometry. Incorporation of C17-PHS is time and concentration dependent, is inhibited by fumonisin B1, an inhibitor of CerS, and greatly reduced in double mutant cells lacking components of the CerS, Lac1 and Lag1. The resulting C17-ceramides are further metabolized to more complex sphingolipids, inositol phosphorylceramide and mannosylinositol phosphorylceramide, indicating that the tracer can be used to decipher the regulation of later steps of the pathway. In support of this notion, we show that mutants lacking the Orm proteins, regulators of the rate-limiting step of the pathway, display increased steady-state levels of these intermediates without affecting their rate of synthesis.—Martínez-Montañés, F., and R. Schneider. Following the flux of long-chain bases through the sphingolipid pathway in vivo using mass spectrometry. *J. Lipid Res.* 2016. 57: 906–915.

**Supplementary key words** ceramide • *Saccharomyces cerevisiae* • ORM proteins

Sphingolipids are greatly enriched in the plasma membrane of eukaryotic cells and they have been implicated in the formation of lateral membrane domains important for the spatial segregations of proteins during their transport to the plasma membrane (1, 2). Whereas animal cells produce sphingolipids in which the ceramide anchor contains a hydrophilic head group composed of choline or carbohydrate moieties, fungi synthesize inositol-containing

sphingolipids, and plants can make of three classes of sphingolipids (3–6).

Sphingolipids and their biosynthetic precursors, long-chain base (LCB) and ceramide, have structural as well as signal functions; their synthesis and turnover thus must be precisely controlled (7). The rate-limiting step of the pathway is under control of serine palmitoyltransferase (SPT), an endoplasmic reticulum (ER)-localized protein complex that catalyzes the condensation of palmitoyl-CoA with serine to yield keto-dihydrosphingosine, a LCB (8). SPT activity is negatively regulated by the Orm proteins, conserved integral ER membrane proteins that form a protein complex together with the phosphoinositide phosphatase, Sac1 (5, 9, 10). Orm proteins are subject to phosphorylation and this relieves their inhibition of SPT activity (9). The kinases that phosphorylate the Orm proteins integrate multiple signals to maintain sphingolipid homeostasis, including heat, ER stress, and nutritional availability via the target of rapamycin (TOR) signaling network (11–15).

After reduction of the 3-keto-dihydrosphingosine to dihydrosphingosine (DHS) and its further hydroxylation to phytosphingosine (PHS), DHS or PHS are converted to ceramide by ceramide synthase (CerS), which catalyzes the formation of an amide bond between the LCB and a C26 very long-chain fatty acid (16, 17). CerS activity is regulated by direct phosphorylation of the catalytic subunits, Lac1 and Lag1, through TORC1, TORC2, and casein kinase 2 (see Fig. 1 for an overview of the pathway and the nomenclature of the intermediates) (15, 18–20).

Ceramide is then converted in the Golgi to inositol phosphorylceramide (IPC), mannosylinositol phosphorylceramide (MIPC), and mannosyl-diinositol phosphorylceramide [M(IP)<sub>2</sub>C] and these complex sphingolipids are transported by vesicular carriers to the plasma membrane,

Abbreviations: Aba, Aureobasidin A; Cer-C, ceramide-C; CerS, ceramide synthase; DHS, dihydrosphingosine; ER, endoplasmic reticulum; FB1, fumonisin B1; IPC, inositol phosphorylceramide; LCB, long-chain base; MIPC, mannosylinositol phosphorylceramide; PHS, phytosphingosine; PtdIns, phosphatidylinositol; SPT, serine palmitoyltransferase; TOR, target of rapamycin.

<sup>1</sup>To whom correspondence should be addressed.

e-mail: roger.schneider@unifr.ch

<sup>S</sup>The online version of this article (available at <http://www.jlr.org>) contains a supplement.

This work was supported by the canton of Fribourg, the Novartis Foundation, and the Swiss National Science Foundation Grant 31003A\_153416.

Manuscript received 11 January 2016 and in revised form 9 March 2016.

Published, JLR Papers in Press, March 14, 2016

DOI 10.1194/jlr.D066472

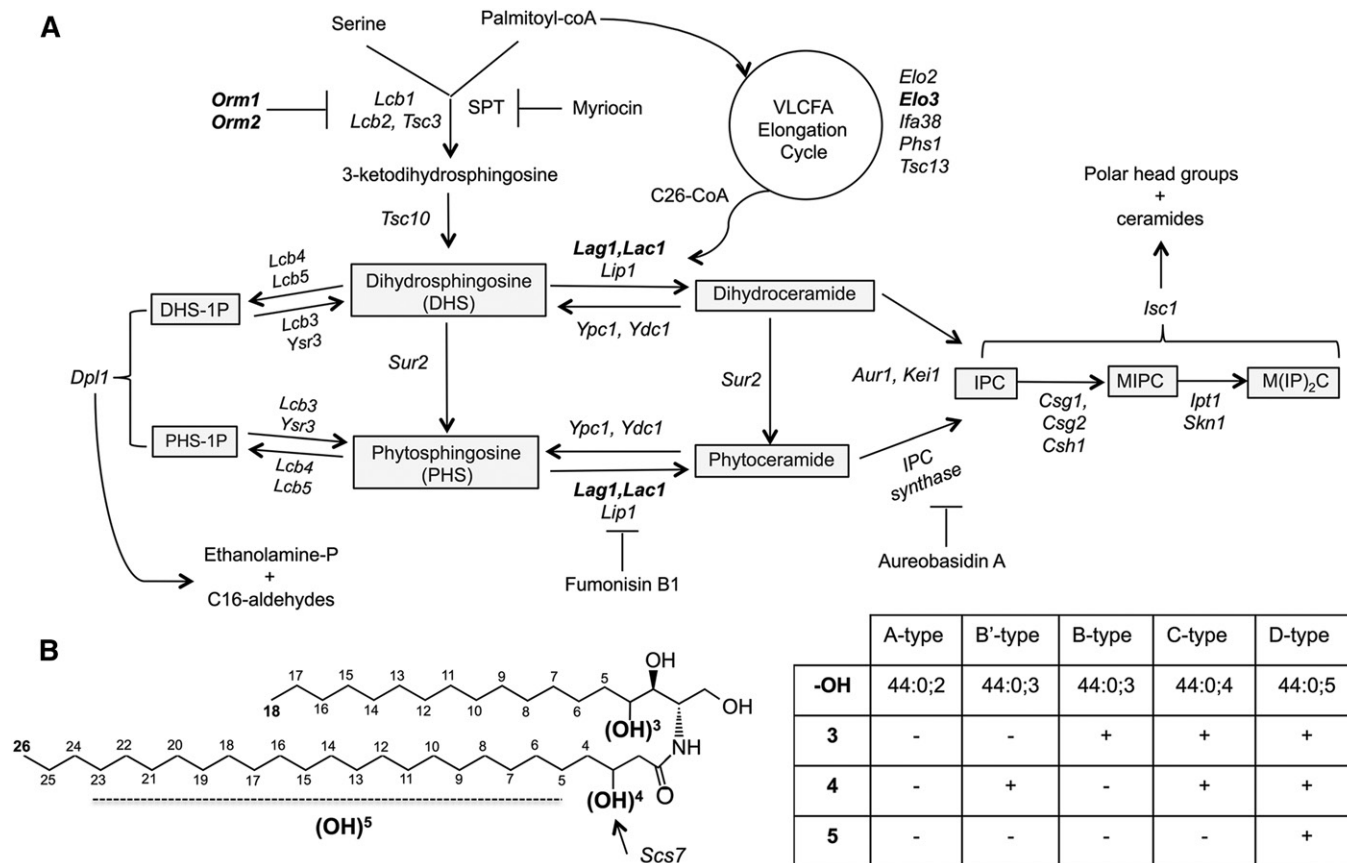


**Fig. 1.** Overview of the sphingolipid biosynthetic pathway. A: Outline of the sphingolipid pathway, important intermediates are boxed, enzymes are italicized, and mutants used in this study are indicated in bold. Drugs that inhibit key steps of the pathway are shown. B: Ceramide structure and nomenclature. The positions of hydroxyl groups on ceramide are indicated and the nomenclature of the corresponding ceramide species is listed in the table.

where they constitute an abundant lipid class of the extracellular leaflet (3, 21–23).

In addition to the biosynthetic pathway, LCBs, ceramide, and complex sphingolipids are subject to a catabolic pathway. LCBs are phosphorylated and then cleaved by the sphingosine-1-phosphate lyase, Dpl1, to ethanolamine phosphate and a fatty aldehyde (24). Ceramide, on the other hand, is degraded through alkaline ceramidases, Ydc1 and Ypc1 (25, 26). Complex sphingolipids are degraded by an inositol phosphosphingolipid phospholipase C, Isc1 (27). The activity of components of the degradative branch, Ydc1, Ypc1, and Isc1, are controlled by the TORC1-Sch9 nutrient signaling pathway (28). Importantly, the transient intermediates of the pathway, LCB, LCB phosphate, and ceramide, not only act as biosynthetic precursors but also have important signaling functions in stress response (29).

To decipher the regulation of key enzymes in the sphingolipid pathway, rapid and reliable determination of their activity and of steady-state levels of intermediates of the pathway is required. For many years radiolabeled substrates, [ $^3\text{H}$ ]labeled LCBs or [ $^{14}\text{C}$ ]labeled acyl-CoAs, followed by separation of the substrates by thin layer chromatography were used to determine CerS activity in vitro (30, 31). IPC synthase activity, on the other hand, was monitored using radiolabeled *N*-acetyl sphinganine (C2-Cer) or radiolabeled

phosphatidylinositol (PtdIns) (32, 33). These isotope-based assays were then replaced by assays using fluorescently labeled lipids. Fluorescently labeled LCBs or fluorescently labeled ceramide have been employed to measure ceramide and IPC synthase activity in vitro (34–36). More recently, the development of lipid mass spectrometry has allowed the use of odd-chain lipids as tracers for in vitro assays (37, 38).

Here we describe a rapid mass spectrometry-based method to determine the flux of LCBs through the sphingolipid pathway in vivo. Using nonnatural odd-chain length C17-DHS or C17-PHS as tracers, we show that C17-LCBs are efficiently taken up, incorporated into ceramide, and further converted to complex sphingolipids, IPC and MIPC, in vivo. These results indicate that C17-LCBs can be used as a tool to decipher the complex regulation of this pathway in vivo.

## MATERIALS AND METHODS

### Yeast strains and growth conditions

Yeast strains and their genotypes are listed in supplementary Table 1. Strains were cultivated in YPD-rich medium [1% Bacto yeast extract, 2% Bacto peptone (USBiological, Swampscott, MA)] or SD synthetic medium [0.67% yeast nitrogen base without

amino acids (USBiological, Salem, MA), 0.73 g/l amino acids] containing 2% glucose. Double-mutant strains were generated by crossing of single mutants and by gene disruption using PCR deletion cassettes and a marker rescue strategy (39). For all lipid tracer experiments, cells were cultivated in YPD at 30°C.

### Lipid extraction and analysis by mass spectrometry

Lipids were extracted from 20 OD units of cells with  $\text{CHCl}_3$  and methanol (17:1 by volume). C17-DHS (1 nmol), PtdIns 17:0/20:4 (0.6 nmol; Avanti Polar Lipids, Alabaster, AL), or C20-ceramide (d18:1/20, 2 nmol; Sigma-Aldrich, St. Louis, MO) were used as internal standards (23). LCBs were analyzed in the positive ion mode and ceramide and complex sphingolipids in the negative ion mode on a Bruker Esquire HCT ion trap mass spectrometer using electrospray ionization at a flow rate of 180 ml/h and a capillary tension of 250 V. Ion fragmentation was induced by argon gas collision at a pressure of 8 mbar.  $[\text{M}+\text{H}]^+$  ions of PHS and  $[\text{M}-\text{H}]^-$  ions of ceramide were quantified relative to internal standards.

For the analysis of complex sphingolipids, lipids were extracted using 95% ethanol, water, diethyl ether, pyridine, and 4.2 N ammonium hydroxide in a ratio of 15:15:5:1:0.18 by volume as described (40, 41). The statistical significance of the data was analyzed by a multiple *t*-test (GraphPad Prism, La Jolla, CA).

## RESULTS AND DISCUSSION

To examine whether C17-LCBs could be used to monitor the activity of the sphingolipid pathway in yeast, cells were first incubated with the odd-chain length lipid tracer for 1 h and lipids were then analyzed by mass spectrometry. In mock-treated cells, the phytoceramide of  $m/z$  710.5 [ceramide-C (Cer-C); 44:0;4 (sum of carbon chain length:number of double bonds:number of hydroxyl groups)] was the most abundant ceramide. Cells that were incubated with C17-PHS (10  $\mu\text{M}$ ), on the other hand, displayed an additional peak at  $m/z$  696.5, expected for a C17-ceramide (43:0;4) (Fig. 2). Fragmentation of the putative C17-containing ceramide yielded a set of negatively charged daughter ions ( $m/z$  411.3 and  $m/z$  365.3) that are diagnostic for C26-fatty acid-containing yeast ceramide. Fragmentation in the positive mode, on the other hand, yielded product ions ( $m/z$  286,  $m/z$  268, and  $m/z$  250) that are characteristic for LCBs, indicating that C17-PHS was indeed incorporated into a C17-ceramide (42) (supplementary Fig. 1).

### C17-PHS is rapidly converted to ceramide

To determine the optimal time of incubation of cells with the C17 tracer, cells were incubated with C17-PHS for increasing periods of time, and the appearance of C17-ceramide was quantified by mass spectrometry. This analysis revealed that the C17 tracer is converted to C17-ceramide within minutes of incubation and that C17-ceramide levels reached a steady-state already after about 30 min of incubation (Fig. 3A). The emergence of constant C17-ceramide levels is likely due to the fact that the C17-ceramide that is produced is efficiently consumed again and converted to more complex sphingolipids, see below.

To examine the concentration-dependence of this conversion, cells were incubated with increasing concentrations of either C17-DHS or C17-PHS and the incorporation of

these tracers into ceramide was monitored. Cells incubated with C17-PHS ranging from 2.5 to 80  $\mu\text{M}$  displayed an almost linear increase in the formation of the fully hydroxylated C17-phytoceramide (43:0;4; Cer-C). Levels of the triple hydroxylated ceramide species (43:0;3; Cer-B) started to increase only when cells were treated with the highest concentration of C17-PHS (80  $\mu\text{M}$ ), suggesting that ceramide hydroxylation becomes rate limiting at very high rates of ceramide formation (Fig. 3B).

Incubation of cells with C17-DHS, on the other hand, revealed a steady concentration-dependent increase of C17-phytoceramide. C17-DHS, however, was also incorporated into dihydroceramide (Cer-B'), albeit with lower efficiency (Fig. 3C). These data indicate that C17-DHS was efficiently hydroxylated to C17-PHS and then incorporated into Cer-C and/or that the C17-DHS containing Cer-B' was efficiently hydroxylated to Cer-C (43). Overall, however, addition of C17-PHS yielded about two times more C17-ceramide than was obtained by the addition of C17-DHS. These differences might be explained by differences in the efficiency of uptake or the incorporation of these two LCB species into ceramide.

### C17-PHS to monitor ceramide synthesis

To test whether the conversion of C17-PHS to C17-phytoceramide could be used to monitor ceramide synthesis *in vivo*, we first examined the concentration-dependent conversion of the C17 tracer in cells that have reduced CerS activity. Cells that have defects in acyl-chain elongation due to a deletion of one component of the elongase complex, *Elo3*, accumulate very-long-chain fatty acids with C24 and C22 instead of the normal C26 carbon atoms. At the same time, *elo3* $\Delta$  mutant cells also accumulate high levels of endogenous PHS, presumably because the C24/C22-CoA acyl chains are not as good as the normal C26-CoA as substrates for ceramide synthesis (44). Consistent with this notion, *elo3* $\Delta$  mutant cells did not show incorporation of C17-PHS into a C26-containing ceramide (Fig. 4A). Instead, they incorporated the C17 tracer into C24-containing ceramide (41:0;4), albeit at lower rates than wild-type cells (Fig. 4B). Note that the levels of C24-phytoceramide in both the wild-type and the *elo3* $\Delta$  mutant are more than 10-fold lower compared with the C26-ceramide levels observed in wild-type cells, suggesting that C24-CoA is poorly incorporated into ceramide.

To assess the role of the sphingolipid  $\alpha$ -hydroxylase, *Scs7*, in the conversion of the triple hydroxylated ceramide species (ceramide-B) to the quadruple hydroxylated species (Cer-C), we examined the incorporation of the C17-LCB tracer in *scs7* $\Delta$  mutant cells (43). Wild-type cells efficiently converted C17-PHS into Cer-C (Fig. 4A) and showed only low levels of ceramide-B; *scs7* $\Delta$  mutant cells accumulated high levels of ceramide-B and could not convert ceramide-B to Cer-C (Fig. 4C).

CerS is composed of two redundant subunits, *Lag1* and *Lac1*, and also contains a nonredundant component, *Lip1* (16, 17, 45). Examination of C17-LCB tracer incorporation into ceramide in a *lag1* $\Delta$  *lac1* $\Delta$  double mutant revealed greatly diminished levels of both ceramide-B and Cer-C

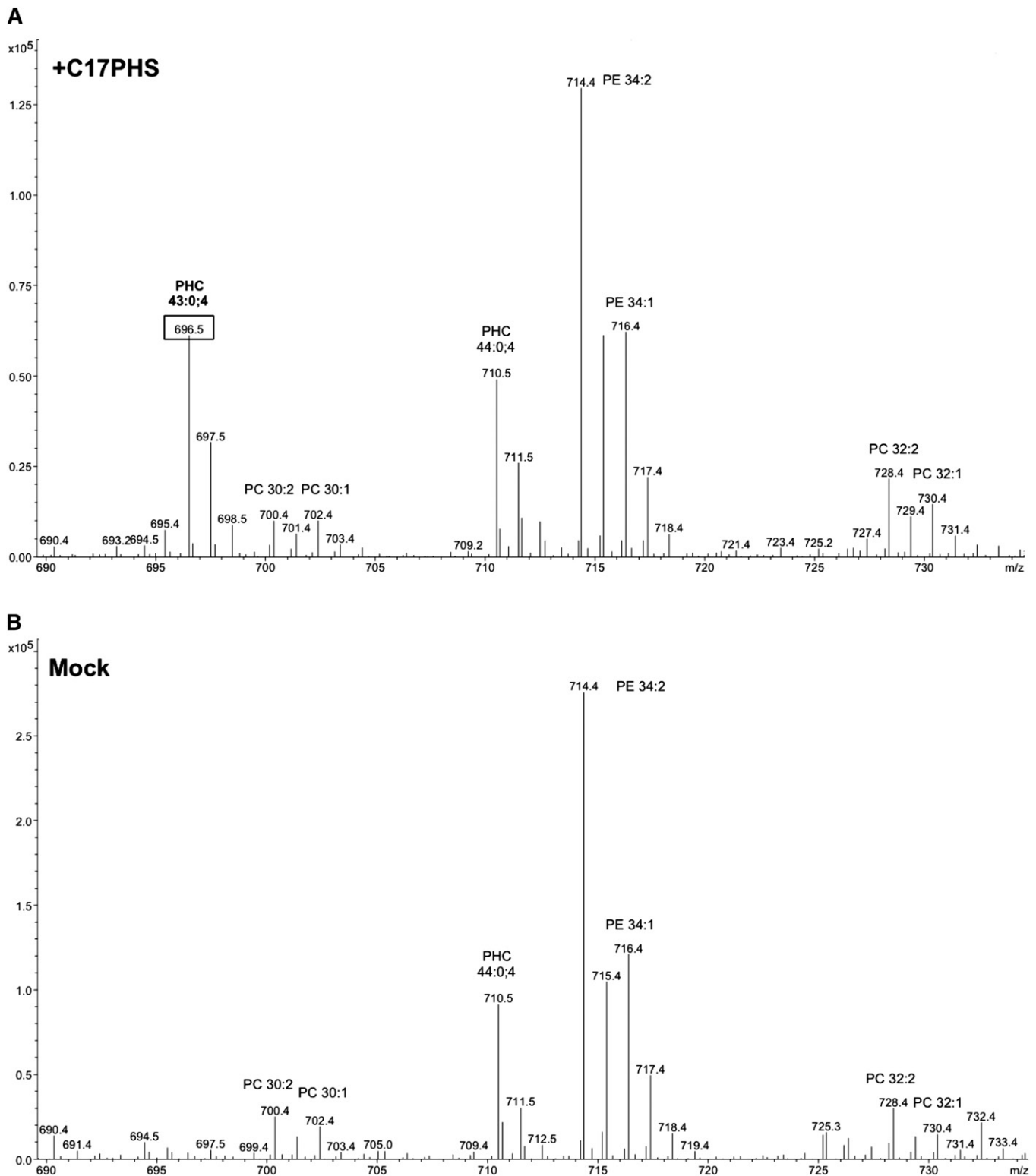


**Fig. 2.** Mass spectra of ceramide species formed from C17-PHS. Lipid profiles of cells incubated with C17-PHS (A) compared with mock-treated cells (B). Cells were incubated with 25  $\mu$ M C17-PHS for 60 min; lipids were extracted and analyzed by mass spectrometry. Relevant lipid species are indicated (PHC, phytoceramide; PC, phosphatidylcholine; PE, phosphatidylethanolamine).

(Fig. 4D). Inhibition of CerS with the mycotoxin, fumonisin B1 (FB1), resulted in decreased levels of newly formed C17-containing ceramide (Cer-C), as well as a dramatic drop in C18-ceramide. These experiments were performed in a *yor1* $\Delta$  mutant, which is deficient in a multidrug transporter

that confers resistance to FB1 (26) (Fig. 4E). On the other hand, treatment of cells with aureobasidin A, which blocks the conversion of ceramide to IPC resulted in accumulation of both types of ceramide, those formed from the endogenous PHS pool as well as ceramide formed by



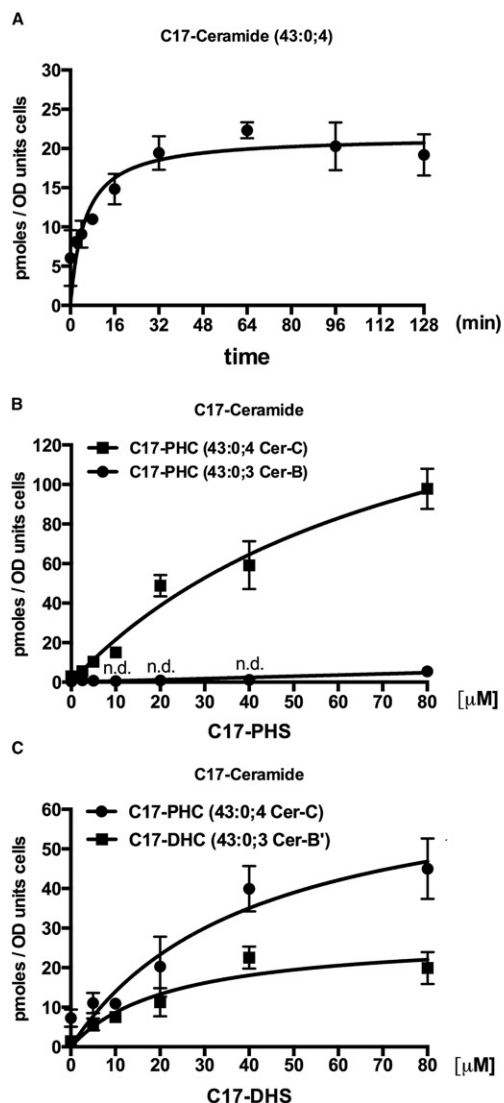


**Fig. 3.** Kinetics of the conversion of C17-LCB into ceramide. Graphs show the time-dependent (A) and concentration-dependent (B) conversion of C17-PHS into ceramide and the concentration-dependent (C) conversion of C17-DHS into phytoceramide [C17-PHC] and dihydroceramide [C17-DHC]. A: Cells were incubated with 10  $\mu$ M of C17-PHS for the indicated period of time, lipids were extracted, and C17-ceramide was quantified by mass spectrometry using C20-ceramide as standard. B, C: Cells were incubated with the indicated concentration of C17-PHS and C17-DHS, respectively, for 30 min and ceramide species were quantified (n.d.; not detectable). Values represent mean  $\pm$  SD of three independent determinations.

the incorporation of the exogenously added C17 tracer (Fig. 4F). Thus, the dual monitoring of the incorporation of natural PHS and the C17 tracer allows discrimination between the differences in ceramide synthesis that are due to defects in the uptake of the tracer and those that are due to reduced incorporation of the LCB into ceramide, i.e., the activity of the CerS.

#### C17-PHS to monitor complex sphingolipid synthesis

To monitor steps downstream of ceramide synthesis, we followed the incorporation of the C17 tracer into complex sphingolipids, IPC and MIPC. Incubation of cells with

50  $\mu$ M C17-PHS resulted in a time-dependent appearance of the tracer in both IPC-C and MIPC-C, and the reaction reached an apparent steady-state after about 60 min (Fig. 5A, B). A higher concentration of the C17 tracer was used in these experiments to increase the yield of downstream products of the pathway and hence improve the signal-to-noise ratio for their detection and quantification. Incorporation of C17-PHS in the complex sphingolipids was concentration dependent, but did not affect the steady-state levels of the endogenous C18-PHS-derived pool of natural IPC and MIPC (Fig. 5C–F). Synthesis of IPC and MIPC from C17-PHS, however, was sensitive to aureobasidin A (Fig. 5G, H).

To analyze the turnover of these lipids, cells were pulsed with C17-PHS; the tracer was then washed out and cells were allowed to grow for various periods of time and C17-containing IPC-C and MIPC were quantified. The results of this analysis indicate that these C17-containing complex sphingolipids are extremely stable because no appreciable decrease in their levels was observed over a 52 h period. These lipids are thus as stable as the natural sphingolipids that were quantified in parallel (supplementary Fig. 2). Taken together, these data indicate that C17-PHS can be used as a tool not only to study the regulation of ceramide synthesis, but also to follow the flux of ceramide through the subsequent steps of the pathway and the turnover of the mature lipids.

#### Orm mutants affect ceramide and IPC levels, but not their synthesis

To test directly whether defects in the homeostatic regulation of the sphingolipid pathway would be detectable with the use of the C17-PHS tracer, we monitored ceramide and complex sphingolipid synthesis in mutants lacking the Orm proteins. These conserved integral membrane proteins of the ER have previously been shown to regulate LCB synthesis (5, 9–15, 19, 20).

In budding yeast, Orm mutant cells accumulate high steady-state levels of LCB, ceramides, and IPC (9, 10). The increased ceramide levels have been attributed to an increased flux of LCB through the pathway (9). Following radiolabeling with serine or DHS, a more recent study observed a decrease in IPC production in the Orm mutant, which was attributed to either a decrease in IPC synthase activity or a reduced transport of ceramide from the ER to the Golgi apparatus, where ceramide is converted to IPC (15). Consistent with the first work, we found that mutant cells lacking both Orm proteins displayed elevated steady-state levels of natural C18-containing ceramides and IPC-C (9) (Fig. 6A). However, incorporation of the C17-PHS tracer into Cer-C and IPC-C was not significantly affected in *orm1 $\Delta$  orm2 $\Delta$*  mutant cells when the concentration of the tracer was kept low (10  $\mu$ M), indicating that the flux of LCB through the pathway is not increased (Fig. 6B). Remarkably, at higher concentrations of C17-PHS (25 and 50  $\mu$ M), wild-type cells displayed a significant increase in Cer-C synthesis. Orm mutant cells, on the other hand, did not respond to these increased levels of C17-PHS (supplementary Fig. 3A). A similar dose-dependent increase was also

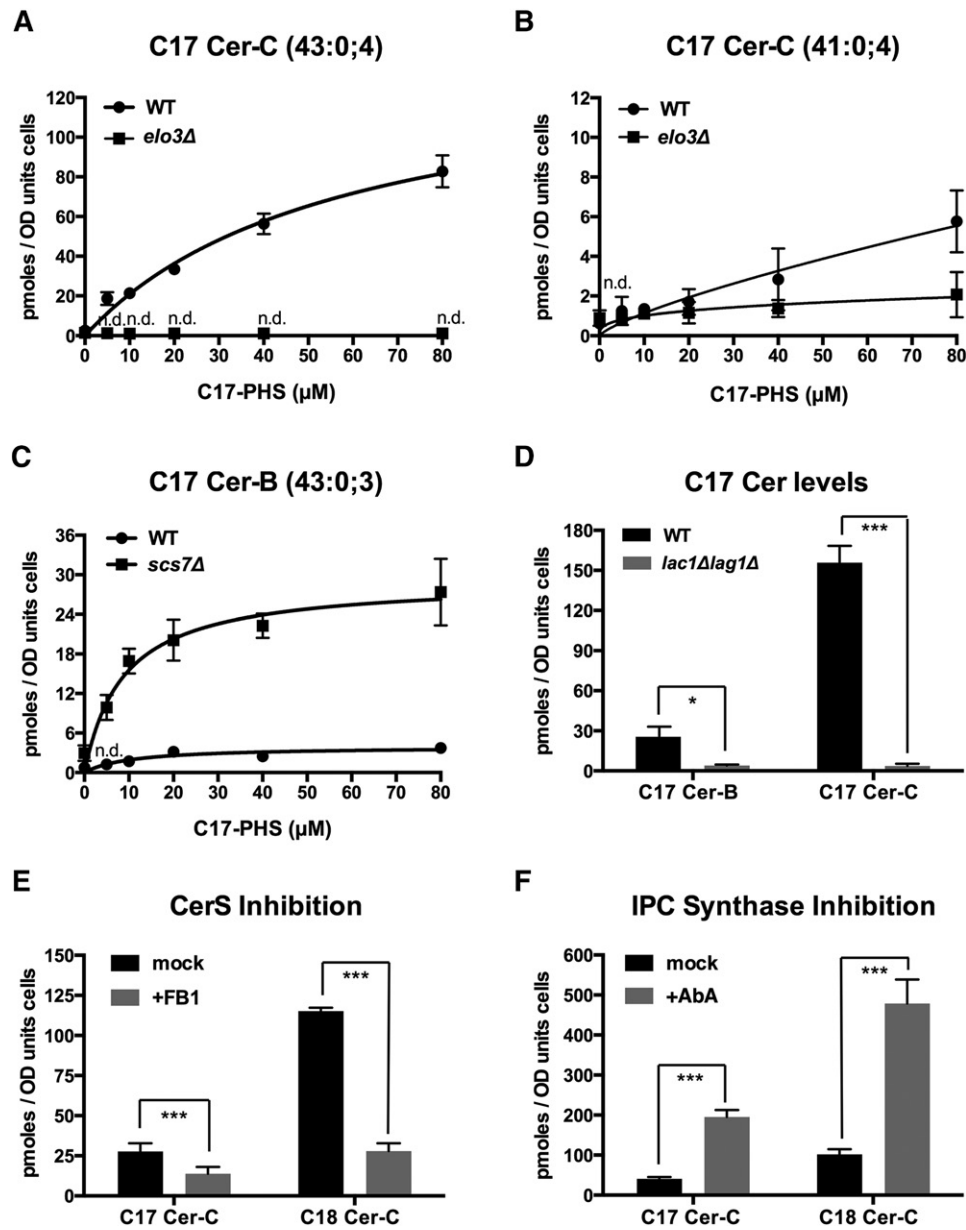


**Fig. 4.** C17-PHS-dependent formation of ceramide is affected in sphingolipid mutants and is sensitive to FB1. A, B: A defect in the synthesis of the C26 fatty acid due to a mutation in the elongase component, Elo3, affects Cer-C production. WT and *elo3Δ* mutant cells were incubated with the indicated concentration of C17-PHS for 30 min and levels of Cer-C with either 43 (A) or 41 carbon atoms (B) were determined. Levels of ceramide containing a full-length C26 fatty acid are undetectable (n.d.) in *elo3Δ* mutant cells, but the mutant and WT cells synthesize low levels of ceramide containing a C24 fatty acid. C: Lack of the sphingolipid  $\alpha$ -hydroxylase, Scs7, results in elevated levels of ceramide-B. WT and *scs7Δ* mutant cells were incubated with the indicated concentration of C17-PHS for 30 min and its incorporation into ceramide-B was determined. D: Synthesis of phytoceramide-B and -C requires the CerS subunits, Lac1 and Lag1. WT and *lag1Δ lac1Δ* double mutant cells were incubated with C17-PHS (50  $\mu$ M, 30 min) and its incorporation into ceramide-B and -C was determined. E: Inhibition of CerS by FB1 reduces the conversion of C17-PHS to Cer-C. Cells lacking the multidrug transporter, Yor1, were treated with FB1 (100  $\mu$ M) overnight, C17-PHS was added (10  $\mu$ M) during 30 min, and both the naturally produced and C17-PHS-derived ceramides were quantified. F: Addition of the IPC synthase inhibitor, aureobasidin A (AbA), results in increased levels of both natural and C17-PHS-derived ceramide. WT cells were treated with aureobasidin A (0.1  $\mu$ g/ml) for 30 min, C17-PHS (50  $\mu$ M) was added for 30 min, and ceramide was quantified. Values represent mean  $\pm$  SD of three independent determinations. Asterisks denote statistical significance (\* $P$  < 0.05; \*\* $P$  < 0.001; \*\*\* $P$  < 0.0001).

observed for IPC-C synthesis (supplementary Fig. 3B). Again, the Orm mutant did not respond to the elevated levels of LCB that were provided. One possible explanation for this apparent lack of substrate-dependent increase

in ceramide and IPC synthesis of Orm mutant cells is the fact that these cells already have greatly elevated steady-state levels of both LCBs and ceramide. High concentrations of exogenously added PHS (20–40  $\mu$ M) inhibit

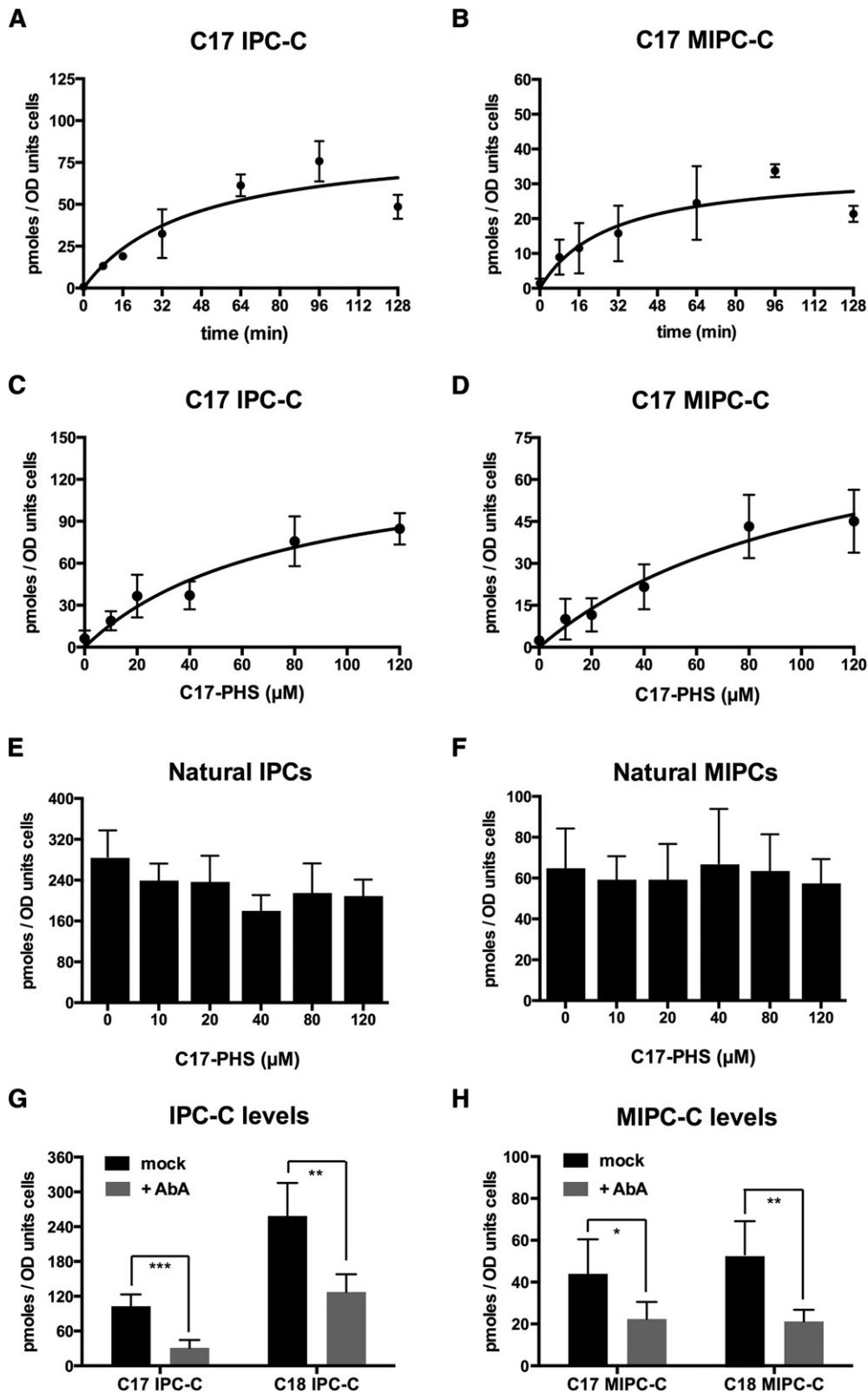


**Fig. 5.** Incorporation of C17-PHS into complex sphingolipids, IPC and MIPC. Graphs show the time- and concentration-dependent incorporation of C17-PHS into IPC (A, C) and MIPC (B, D). The addition of the C17-PHS tracer does not affect levels of C18-PHS-derived natural IPC-C and MIPC. Levels of natural complex sphingolipids, IPC-C (E) and MIPC (F), were determined in cells incubated with the indicated concentration of C17-PHS for 30 min. IPC and MIPC levels were decreased upon addition of aureobasidin A (AbA). G, H: Cells were incubated with aureobasidin A (0.1  $\mu$ g/ml) for 30 min, C17-PHS was added (50  $\mu$ M) for 45 min before lipids were extracted and IPC (G) and MIPC (H) levels were quantified. Values represent mean  $\pm$  SD of three independent determinations. Asterisks denote statistical significance (\* $P$  < 0.05; \*\* $P$  < 0.001; \*\*\* $P$  < 0.0001).

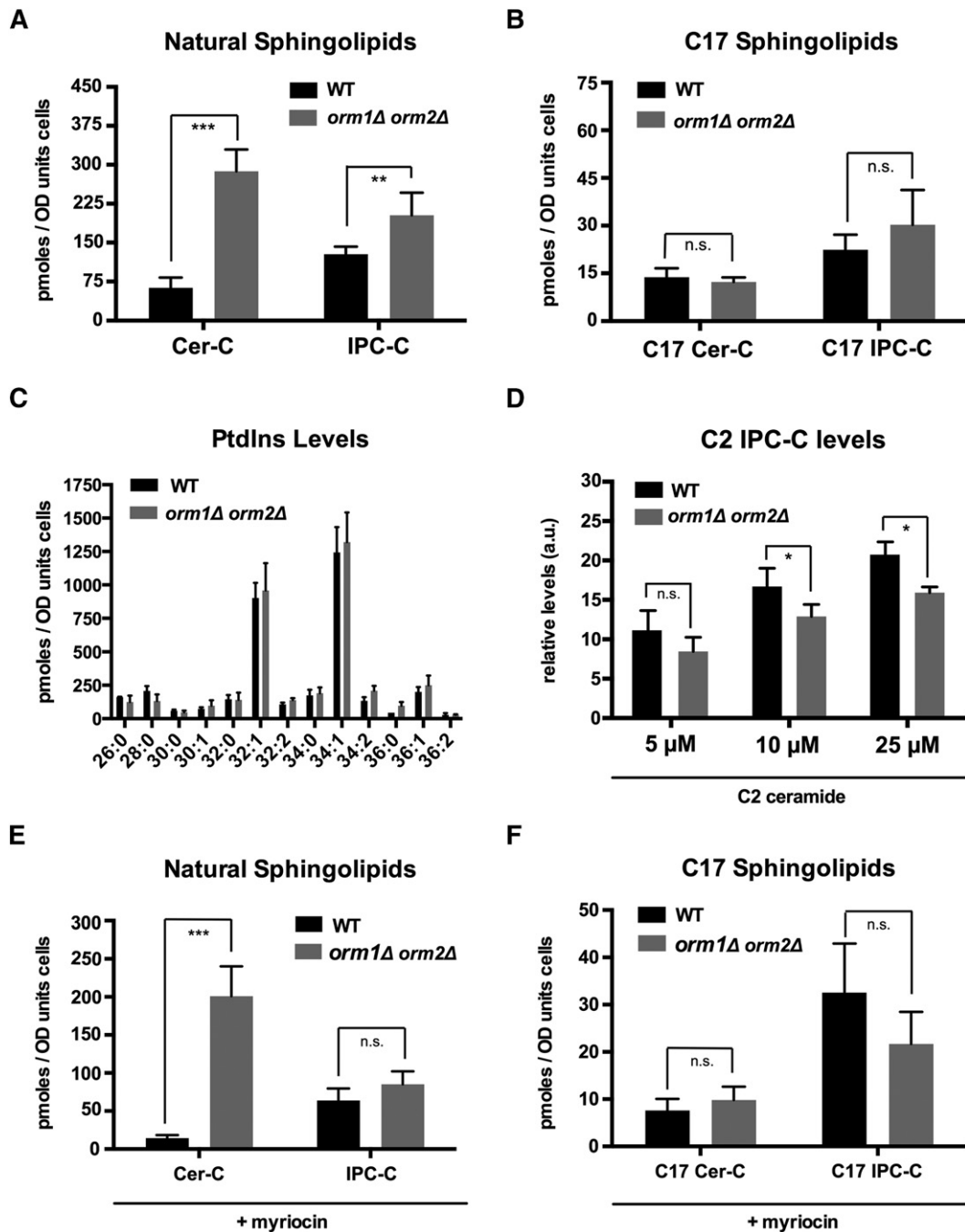


**Fig. 6.** Orm proteins affect ceramide and IPC levels but not their rate of synthesis. **A:** Steady-state levels of natural ceramide and IPC are elevated in Orm double mutant cells. Cer-C and IPC-C levels were quantified in the same samples as shown in (B). **B:** Lack of Orm function does not affect ceramide and IPC synthesis. WT and *orm1Δ orm2Δ* double mutant cells were incubated with C17-PHS (10 μM) for 30 min and incorporation of the tracer into ceramide and IPC-C was quantified. **C:** Levels of PtdIns are not affected in cells lacking Orm. PtdIns levels were quantified using PtdIns (17:0/20:4) as nonnatural internal standard. **D:** Lack of Orm function does not significantly affect IPC synthesis. Cells were incubated with the soluble C2-ceramide analog (5, 10, and 25 μM) for 30 min and its incorporation into IPC-C was quantified. **E, F:** Lack of Orm function does not affect ceramide and IPC synthesis in myriocin-treated cells. WT and Orm mutant cells were preincubated with myriocin (1 μg/ml) for 1.5 h and C17-PHS (10 μM) was then added for 30 min before natural (E) and newly synthesized (F) ceramides and IPC-C were quantified. Values represent mean ± SD of at least three independent determinations. Asterisks denote statistical significance (\* $P < 0.05$ ; \*\* $P < 0.001$ ; \*\*\* $P < 0.0001$ ).

cell cycle progression (46). With their elevated levels of intracellular PHS and ceramide, Orm mutant cells might be hypersensitive to this PHS-mediated cell cycle arrest.

Levels of PtdIns, a cosubstrate for the synthesis of IPC by Aur1, were not affected in the Orm mutant (Fig. 6C). To further confirm that elevated levels of ceramide in the Orm mutant cells were not due to decreased IPC synthase




activity, we incubated cells with the soluble C2-ceramide and monitored its incorporation into C2-IPC. Cells lacking Orm function did not show a significantly decreased incorporation of C2-ceramide into IPC when incubated with low concentrations of C2-ceramide (5  $\mu\text{M}$ ), indicating that IPC synthase activity is not affected (Fig. 6D). However, at higher concentrations of C2-ceramide (10  $\mu\text{M}$ ), the Orm mutant again displayed a slight, but significant, reduction in IPC-C synthesis and this was even more pronounced when 25  $\mu\text{M}$  C2-ceramide was provided to the cells (Fig. 6D). This concentration-dependent inhibition of IPC synthesis in the Orm mutant might again be explained by a higher sensitivity to C2-ceramide-mediated cell cycle inhibition due to the greatly elevated steady-state levels of ceramide that these cells have (47).

Because labeling with radiolabeled serine and DHS is typically performed with cells grown in synthetic media, whereas the data provided here were obtained from cells grown in rich media, we wondered whether differences in media compositions affect steady-state levels of ceramide and IPC-C and whether they also impact on the rate of ceramide and IPC synthesis. The media composition, particularly serine levels, is known to affect the rate of LCB synthesis (48, 49). In comparison to wild-type cells, Orm mutant cells had elevated levels of ceramide and IPC-C when cultivated in rich media (YPD) (Fig. 6A; supplementary Fig. 4A, B). In synthetic media, however, these differences were not significant, explaining discrepancies in ceramide levels of Orm mutant cells reported before (9, 10). The rate of ceramide and IPC synthesis in wild-type and Orm mutant cells was comparable, independent of whether the cells were grown in rich or synthetic media (Fig. 6B; supplementary Fig. 4C, D).

To explore whether elevated LCB levels in Orm mutant cells negatively affect ceramide synthesis, we pharmacologically reduced SPT activity and thereby the steady-state levels of PHS and ceramide, by using myriocin. Wild-type and Orm mutant cells treated with the drug showed a similar incorporation of the tracer into C17-ceramide and C17-IPC-C as the nontreated cells, indicating that the elevated LCB and ceramide levels in the Orm mutant cells do not inhibit ceramide and IPC synthesis when low concentrations of the C17 tracer (10  $\mu\text{M}$ ) are used (Fig. 6E, F). Taken together, these data indicate that Orm mutant cells do not have an increased flux through the pathway because both de novo synthesis of ceramide and that of IPC-C occur with a rate that is comparable to that of wild-type cells. Nevertheless, these cells accumulate ceramide and IPC when cultivated in rich media, suggesting that the turnover of these intermediates may be reduced in the absence of Orm function.

In agreement with this possibility, treatment of Orm mutant cells with myriocin for 2 h did not completely reverse ceramide accumulation (Fig. 6E). Thus, a reduced ceramidase activity or an increased degradation of complex sphingolipids, exerted by Isc1, the yeast ortholog of mammalian neutral sphingomyelinase type 2, might contribute to the elevated steady-state pool of ceramide in the Orm mutant. In support of this possibility, Orm2 and Isc1 display

negative genetic interactions with each other (50). Alternatively, Orm proteins may affect the localization, expression, and/or activity of Lcb4, the major LCB kinase in yeast. Reduced activity of Lcb4 would, on one hand, result in reduced degradation of LCBs and thereby increase the half-life of its internal pool. On the other hand, Lcb4 activity affects phosphorylation of exogenously added PHS, a prerequisite for its incorporation into ceramides (51).

Taken together, the data provided here establish proof of principle that C17-PHS can serve as a useful tool to monitor the activity of multiple enzymes in the sphingolipid pathway in vivo, to monitor the flux of substrates through the pathway, and to decipher the regulation of key enzymes within the pathway. As exemplified by the analysis of the Orm mutant, the use of this odd-chain length precursor has the added advantage that both steady-state levels of the normally produced C18-containing lipids as well as the time-dependent production of newly formed C17-containing intermediates of the sphingolipid pathway can be monitored simultaneously. 

The authors thank members of the laboratory for their support, A. Conzelmann for helpful discussions, and Stéphanie Cottier for comments on the manuscript.

## REFERENCES

- Lingwood, D., and K. Simons. 2010. Lipid rafts as a membrane-organizing principle. *Science*. **327**: 46–50.
- Holthuis, J. C., and A. K. Menon. 2014. Lipid landscapes and pipelines in membrane homeostasis. *Nature*. **510**: 48–57.
- Dickson, R. C. 2008. New insights into sphingolipid metabolism and function in budding yeast. *J. Lipid Res.* **49**: 909–921.
- Bartke, N., and Y. A. Hannun. 2009. Bioactive sphingolipids: metabolism and function. *J. Lipid Res.* **50**(Suppl): S91–S96.
- Breslow, D. K., and J. S. Weissman. 2010. Membranes in balance: mechanisms of sphingolipid homeostasis. *Mol. Cell.* **40**: 267–279.
- Markham, J. E., D. V. Lynch, J. A. Napier, T. M. Dunn, and E. B. Cahoon. 2013. Plant sphingolipids: function follows form. *Curr. Opin. Plant Biol.* **16**: 350–357.
- Hannun, Y. A., and L. M. Obeid. 2008. Principles of bioactive lipid signalling: lessons from sphingolipids. *Nat. Rev. Mol. Cell Biol.* **9**: 139–150.
- Hanada, K. 2003. Serine palmitoyltransferase, a key enzyme of sphingolipid metabolism. *Biochim. Biophys. Acta.* **1632**: 16–30.
- Breslow, D. K., S. R. Collins, B. Bodenmiller, R. Aebersold, K. Simons, A. Shevchenko, C. S. Ejsing, and J. S. Weissman. 2010. Orm family proteins mediate sphingolipid homeostasis. *Nature*. **463**: 1048–1053.
- Han, S., M. A. Lone, R. Schnleiter, and A. Chang. 2010. Orm1 and Orm2 are conserved endoplasmic reticulum membrane proteins regulating lipid homeostasis and protein quality control. *Proc. Natl. Acad. Sci. USA.* **107**: 5851–5856.
- Roelants, F. M., D. K. Breslow, A. Muir, J. S. Weissman, and J. Thorner. 2011. Protein kinase Ypk1 phosphorylates regulatory proteins Orm1 and Orm2 to control sphingolipid homeostasis in *Saccharomyces cerevisiae*. *Proc. Natl. Acad. Sci. USA.* **108**: 19222–19227.
- Liu, M., C. Huang, S. R. Polu, R. Schnleiter, and A. Chang. 2012. Regulation of sphingolipid synthesis through Orm1 and Orm2 in yeast. *J. Cell Sci.* **125**: 2428–2435.
- Sun, Y., Y. Miao, Y. Yamane, C. Zhang, K. M. Shokat, H. Takematsu, Y. Kozutsumi, and D. G. Drubin. 2012. Orm protein phosphoregulation mediates transient sphingolipid biosynthesis response to heat stress via the Pkh-Ypk and Cdc55-PP2A pathways. *Mol. Biol. Cell.* **23**: 2388–2398.

14. Gururaj, C., R. S. Federman, R. Federman, and A. Chang. 2013. Orm proteins integrate multiple signals to maintain sphingolipid homeostasis. *J. Biol. Chem.* **288**: 20453–20463. [Erratum. 2015. *J. Biol. Chem.* **290**: 1455.]
15. Shimobayashi, M., W. Oppliger, S. Moes, P. Jenö, and M. N. Hall. 2013. TORC1-regulated protein kinase Npr1 phosphorylates Orm to stimulate complex sphingolipid synthesis. *Mol. Biol. Cell.* **24**: 870–881.
16. Guillas, I., P. A. Kirchman, R. Chuard, M. Pfefferli, J. C. Jiang, S. M. Jazwinski, and A. Conzelmann. 2001. C26-CoA-dependent ceramide synthesis of *Saccharomyces cerevisiae* is operated by Lag1p and Lac1p. *EMBO J.* **20**: 2655–2665.
17. Schorling, S., B. Vallee, W. P. Barz, H. Riezman, and D. Oesterhelt. 2001. Lag1p and Lac1p are essential for the acyl-CoA-dependent ceramide synthase reaction in *Saccharomyces cerevisiae*. *Mol. Biol. Cell.* **12**: 3417–3427.
18. Kobayashi, S. D., and M. M. Nagiec. 2003. Ceramide/long-chain base phosphate rheostat in *Saccharomyces cerevisiae*: regulation of ceramide synthesis by Elo3p and Cka2p. *Eukaryot. Cell.* **2**: 284–294.
19. Muir, A., S. Ramachandran, F. M. Roelants, G. Timmons, and J. Thorner. 2014. TORC2-dependent protein kinase Ypk1 phosphorylates ceramide synthase to stimulate synthesis of complex sphingolipids. *eLife.* **3**: e03799.
20. Fresques, T., B. Niles, S. Aronova, H. Mogri, T. Rakhshandehroo, and T. Powers. 2015. Regulation of ceramide synthase by casein kinase 2-dependent phosphorylation in *Saccharomyces cerevisiae*. *J. Biol. Chem.* **290**: 1395–1403.
21. Puoti, A., C. Desponds, and A. Conzelmann. 1991. Biosynthesis of mannosylinositolphosphoceramide in *Saccharomyces cerevisiae* is dependent on genes controlling the flow of secretory vesicles from the endoplasmic reticulum to the Golgi. *J. Cell Biol.* **113**: 515–525.
22. Funato, K., and H. Riezman. 2001. Vesicular and nonvesicular transport of ceramide from ER to the Golgi apparatus in yeast. *J. Cell Biol.* **155**: 949–959.
23. Ejsing, C. S., J. L. Sampaio, V. Surendranath, E. Duchoslav, K. Ekroos, R. W. Klemm, K. Simons, and A. Shevchenko. 2009. Global analysis of the yeast lipidome by quantitative shotgun mass spectrometry. *Proc. Natl. Acad. Sci. USA.* **106**: 2136–2141.
24. Saba, J. D., F. Nara, A. Bielawska, S. Garrett, and Y. A. Hannun. 1997. The BST1 gene of *Saccharomyces cerevisiae* is the sphingosine-1-phosphate lyase. *J. Biol. Chem.* **272**: 26087–26090.
25. Mao, C., R. Xu, A. Bielawska, Z. M. Szulc, and L. M. Obeid. 2000. Cloning and characterization of a *Saccharomyces cerevisiae* alkaline ceramidase with specificity for dihydroceramide. *J. Biol. Chem.* **275**: 31369–31378.
26. Mao, C., R. Xu, A. Bielawska, and L. M. Obeid. 2000. Cloning of an alkaline ceramidase from *Saccharomyces cerevisiae*. An enzyme with reverse (CoA-independent) ceramide synthase activity. *J. Biol. Chem.* **275**: 6876–6884.
27. Sawai, H., Y. Okamoto, C. Luberto, C. Mao, A. Bielawska, N. Domae, and Y. A. Hannun. 2000. Identification of ISCI (YER019w) as inositol phosphosphingolipid phospholipase C in *Saccharomyces cerevisiae*. *J. Biol. Chem.* **275**: 39793–39798.
28. Swinnen, E., T. Wilms, J. Idkowiak-Baldys, B. Smets, P. De Snijder, S. Accardo, R. Ghillebert, K. Thevissen, B. Cammue, D. De Vos, et al. 2014. The protein kinase Sch9 is a key regulator of sphingolipid metabolism in *Saccharomyces cerevisiae*. *Mol. Biol. Cell.* **25**: 196–211.
29. Epstein, S., and H. Riezman. 2013. Sphingolipid signaling in yeast: potential implications for understanding disease. *Front. Biosci. (Elite Ed.)* **5**: 97–108.
30. Lahiri, S., H. Lee, J. Mesicek, Z. Fuks, A. Haimovitz-Friedman, R. N. Kolesnick, and A. H. Futerman. 2007. Kinetic characterization of mammalian ceramide synthases: determination of K(m) values towards sphinganine. *FEBS Lett.* **581**: 5289–5294.
31. Mizutani, Y., A. Kihara, and Y. Igarashi. 2005. Mammalian Lass6 and its related family members regulate synthesis of specific ceramides. *Biochem. J.* **390**: 263–271.
32. Nagiec, M. M., E. E. Nagiec, J. A. Baltisberger, G. B. Wells, R. L. Lester, and R. C. Dickson. 1997. Sphingolipid synthesis as a target for antifungal drugs. Complementation of the inositol phosphorylceramide synthase defect in a mutant strain of *Saccharomyces cerevisiae* by the AUR1 gene. *J. Biol. Chem.* **272**: 9809–9817.
33. Ko, J., S. Cheah, and A. S. Fischl. 1994. Regulation of phosphatidylinositol:ceramide phosphoinositol transferase in *Saccharomyces cerevisiae*. *J. Bacteriol.* **176**: 5181–5183.
34. Zhong, W., D. J. Murphy, and N. H. Georgopapadakou. 1999. Inhibition of yeast inositol phosphorylceramide synthase by aureobasidin A measured by a fluorometric assay. *FEBS Lett.* **463**: 241–244.
35. Kim, H. J., Q. Qiao, H. D. Toop, J. C. Morris, and A. S. Don. 2012. A fluorescent assay for ceramide synthase activity. *J. Lipid Res.* **53**: 1701–1707.
36. Tidhar, R., K. Sims, E. Rosenfeld-Gur, W. Shaw, and A. H. Futerman. 2015. A rapid ceramide synthase activity using NBD-sphinganine and solid phase extraction. *J. Lipid Res.* **56**: 193–199.
37. Spassieva, S., J. G. Seo, J. C. Jiang, J. Bielawski, F. Alvarez-Vasquez, S. M. Jazwinski, Y. A. Hannun, and L. M. Obeid. 2006. Necessary role for the Lag1p motif in (dihydro)ceramide synthase activity. *J. Biol. Chem.* **281**: 33931–33938.
38. Schulz, A., T. Mousallem, M. Venkataramani, D. A. Persaud-Sawin, A. Zucker, C. Luberto, A. Bielawska, J. Bielawski, J. C. Holthuis, S. M. Jazwinski, et al. 2006. The CLN9 protein, a regulator of dihydroceramide synthase. *J. Biol. Chem.* **281**: 2784–2794.
39. Gueldener, U., J. Heinisch, G. J. Koehler, D. Voss, and J. H. Hegemann. 2002. A second set of loxP marker cassettes for Cre-mediated multiple gene knockouts in budding yeast. *Nucleic Acids Res.* **30**: e23.
40. Guan, X. L., I. Riezman, M. R. Wenk, and H. Riezman. 2010. Yeast lipid analysis and quantification by mass spectrometry. *Methods Enzymol.* **470**: 369–391.
41. Angus, W. W., and R. L. Lester. 1972. Turnover of inositol and phosphorus containing lipids in *Saccharomyces cerevisiae*; extracellular accumulation of glycerophosphorylinositol derived from phosphatidylinositol. *Arch. Biochem. Biophys.* **151**: 483–495.
42. Ejsing, C. S., T. Moehring, U. Bahr, E. Duchoslav, M. Karas, K. Simons, and A. Shevchenko. 2006. Collision-induced dissociation pathways of yeast sphingolipids and their molecular profiling in total lipid extracts: a study by quadrupole TOF and linear ion trap-orbitrap mass spectrometry. *J. Mass Spectrom.* **41**: 372–389.
43. Haak, D., K. Gable, T. Beeler, and T. Dunn. 1997. Hydroxylation of *Saccharomyces cerevisiae* ceramides requires Sur2p and Scs7p. *J. Biol. Chem.* **272**: 29704–29710.
44. Oh, C. S., D. A. Toke, S. Mandala, and C. E. Martin. 1997. ELO2 and ELO3, homologues of the *Saccharomyces cerevisiae* ELO1 gene, function in fatty acid elongation and are required for sphingolipid formation. *J. Biol. Chem.* **272**: 17376–17384.
45. Vallée, B., and H. Riezman. 2005. Lip1p: a novel subunit of acyl-CoA ceramide synthase. *EMBO J.* **24**: 730–741.
46. Jenkins, G. M., and Y. A. Hannun. 2001. Role for de novo sphingoid base biosynthesis in the heat-induced transient cell cycle arrest of *Saccharomyces cerevisiae*. *J. Biol. Chem.* **276**: 8574–8581.
47. Nickels, J. T., and J. R. Broach. 1996. A ceramide-activated protein phosphatase mediates ceramide-induced G1 arrest of *Saccharomyces cerevisiae*. *Genes Dev.* **10**: 382–394.
48. Cowart, L. A., and Y. A. Hannun. 2007. Selective substrate supply in the regulation of yeast de novo sphingolipid synthesis. *J. Biol. Chem.* **282**: 12330–12340.
49. Montefusco, D. J., B. Newcomb, J. L. Gandy, S. E. Brice, N. Matmati, L. A. Cowart, and Y. A. Hannun. 2012. Sphingoid bases and the serine catabolic enzyme CHA1 define a novel feedforward/feedback mechanism in the response to serine availability. *J. Biol. Chem.* **287**: 9280–9289.
50. Hoppins, S., S. R. Collins, A. Cassidy-Stone, E. Hummel, R. M. Devay, L. L. Lackner, B. Westermann, M. Schuldiner, J. S. Weissman, and J. Nunnari. 2011. A mitochondrial-focused genetic interaction map reveals a scaffold-like complex required for inner membrane organization in mitochondria. *J. Cell Biol.* **195**: 323–340.
51. Funato, K., R. Lombardi, B. Vallee, and H. Riezman. 2003. Lcb4p is a key regulator of ceramide synthesis from exogenous long chain sphingoid base in *Saccharomyces cerevisiae*. *J. Biol. Chem.* **278**: 7325–7334.